Coexistence of polaronic and band states in a bilayer manganite from two-dimensional reconstruction of magnetic Compton profiles

Akihisa Koizumi,[1] Toshihiro Nagao,[1] Nobuhiko Sakai,[1] Kazuma Hirota,[2] and Yoich Murakami[3]
[1]*Graduate School of Material Science, University of Hyogo, Kamigori, Ako-gun, Hyogo 678-1297, Japan*
[2]*Neutron Science Laboratory, Institute for Solid State Physics, University of Tokyo, Naka-gun, Ibaragi 319-1106, Japan*
[3]*Graduate School of Science, Tohoku University, Sendai, Miyagi 980-8578, Japan*
(Received 20 April 2006; revised manuscript received 21 June 2006; published 25 July 2006)

We have measured directional magnetic Compton profiles between [100] and [110] directions in a bilayer manganite at 10 K. The two-dimensional spin momentum distribution of the Mn 3*d* state is reconstructed from them. The result is examined in both terms of molecular orbital and band schemes. The e_g type orbitals are dominated by the x^2-y^2 type orbital. The occupation-number density in the *k* space obtained by the Lock-Crisp-West folding is not explained only by the band picture, and suggests that a polaronic state of e_g type electrons coexists in the ferromagnetic metal phase below T_c.

DOI: 10.1103/PhysRevB.74.012408 PACS number(s): 75.47.Lx, 71.38.−k, 75.47.Gk, 78.70.Ck

The perovskite manganites have provided intriguing subjects since the discovery of colossal magnetoresistance (CMR) phenomenon observed above a metal-insulator (MI) transition temperature, T_c.[1] In addition, the manganites show a complicated magnetic phase diagram, charge and orbital orderings.[2] The Mn 3*d* electronic state, which is split into e_g and t_{2g} orbitals in the octahedral crystal field of MnO_6, will be responsible for the physical properties. So far, the ferromagnetic metal (FM) phase below T_c has been explained based on the double-exchange (DE) mechanism where the spin degree of freedom is taken into account.[3] Through the past experimental and theoretical investigations on the manganites, the importance of the orbital degree of freedom, which should be closely correlated with the lattice degree of freedom, has been recognized as well as charge and spin ones.[4] Recently, Ramakrishnan *et al.* have proposed a new theoretical model where a polaronic and broadband e_g states coexist in the FM phase, and systematically explained the MI transition and the CMR effect.[5] Miyaki *et al.* have also pointed out the possibility of the coexisting state in another theoretical approach.[6] In accord with the theoretical works, information of the e_g orbital state involved with the Jahn-Teller coupling and electron correlation effects will be a central issue to understand the physical properties of this system. In the study of orbital physics on the manganites, magnetic Compton-profile (MCP) measurements have been successfully employed to elucidate the orbital occupancy.[7–9] In this paper, we report on the itinerant and localized features of the e_g orbital state through the two-dimensional spin momentum distribution (2D-SMD) reconstructed from several 1D MCP's measured in a single crystal of ferromagnetic $La_{2-2x}Sr_{1+2x}Mn_2O_7$ ($x=0.35$) at 10 K. The 2D-SMD is examined from viewpoints of *k*-space wave functions derived both from molecular orbital and band calculations. The result suggests the coexistence of polaronic and band states of e_g type electrons.

Within the framework of the impulse approximation, MCP, $J_{mag}(p_z)$, is defined as

$$J_{mag}(p_z) = \int\int \left(\sum_i |\chi_{i\uparrow}(\mathbf{p})|^2 - \sum_j |\chi_{j\downarrow}(\mathbf{p})|^2 \right) dp_x dp_y, \quad (1)$$

where p_z is an electron momentum component in the direction of the scattering vector of x rays.[10] The $\chi_{i\uparrow(\downarrow)}(\mathbf{p})$ is a *k*-space wave function of the *i*th electron with up-spin (down-spin) in the initial state. The subscripts *i* and *j* go through all occupied states.

The area of a MCP is proportional to the magnitude of the spin magnetic moment in a ferromagnetic material, hence we can evaluate electron numbers of occupied states. In addition, as shown by Eq. (1), MCP directly reflects the wave functions of magnetic electrons in the form of the double integral of the difference in momentum density, $|\chi_i(\mathbf{p})|^2$, between spin-up and spin-down electrons with respect to p_x and p_y. Therefore, its shape directly depends both on the orbitals occupied by magnetic electrons and observation directions. If MCP's are measured on a single crystal in many directions, a 2D or 3D-SMD can be reconstructed from them, resulting in the visualization of occupied states by magnetic electrons. Although such a reconstruction study of MCP's has been performed only on a typical ferromagnet Fe,[11] recent progress of the synchrotron-radiation technique has made it more practical.

The single crystal of $La_{2-2x}Sr_{1+2x}Mn_2O_7$ ($x=0.35$) was melt-grown in a flowing oxygen gas in a floating zone optical image furnace.[12] This system has a nearly two-dimensional Brillouin zone because of a structural feature where a MnO_2 bilayer and a $(La,Sr)_2O_2$ blocking layer are alternately piled up along the *c* axis. According to the magnetic phase diagram obtained by neutron-diffraction measurements, the present sample shows in-plane ferromagnetism below T_c that was determined to be 125 K from magnetic susceptibility measurement.

MCP's were measured on the beam line 08 W at SPring-8, Japan. Elliptically polarized x rays emitted from an elliptical multipole wiggler were monochromatized to 175 keV and incident on the sample. The scattered x rays

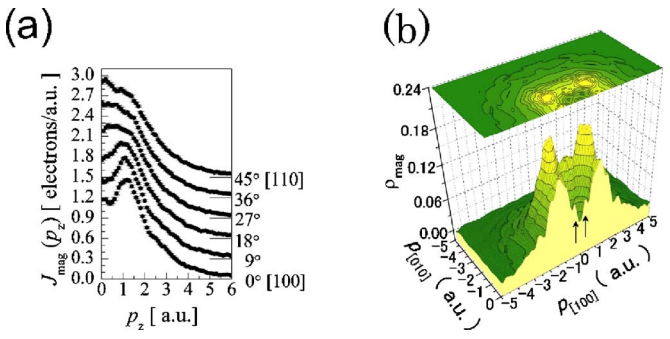

FIG. 1. (Color online) MCP's and 2D-SMD. (a) Directional MCP's measured between the [100] and [110] axes at intervals of 9°. The error bars indicate experimental statistical errors. (b) 2D-SMD projected on the (001) plane through the reconstruction analysis of the MCP's. The 2D-SMD was obtained by the expansion of the measured area according to the structural symmetry.

with a scattering angle of 178.5° were energy analyzed by a 10-segmented Ge solid state detector. During the measurement, an external magnetic field of ±2.5 T was alternately applied along the measuring direction to reverse magnetization in the sample. Each MCP was extracted as the difference between the two Compton profiles measured on the same sample magnetized in the opposite directions with a fixed photon helicity.

Figure 1(a) shows MCP's measured between the [100] and [110] crystal axes at intervals of 9°. Each MCP was corrected for sample absorption, scattering cross section, and detection efficiency, and was folded at the origin and averaged. The abscissa p_z is taken to be parallel to each measuring direction, and is represented in atomic units (a.u.). The overall momentum resolution was 0.45 a.u. in the present measurement. The change in MCP reflects the orbital structure consisting of t_{2g} and e_g orbital contributions with weighting factors of respective spin magnetic moments. Figure 1(b) shows a 2D-SMD reconstructed from the MCP's. The reconstruction analysis used here was the direct Fourier-transform method.[13] Each MCP in Fig. 1(a) was once Fourier-transformed into a one-dimensional function $B(r)$. Then, the interspaces between these functions are interpolated to obtain a 2D or 3D $B(\mathbf{r})$ function, the so-called reciprocal form factor. The inverse Fourier transform of $B(\mathbf{r})$ provides the momentum density $\rho(\mathbf{p})$ of magnetic electrons. In the case of two-dimensional reconstruction, what one obtains is equivalent to the integration of momentum density with respect to the direction perpendicular to a view plane, $\rho(p_x,p_y)=\int\rho(\mathbf{p})dp_z$. Therefore, Fig. 1(b) corresponds to the projection of the spin momentum density of Mn-3d orbitals on the (001) plane. The concaves around ±2 a.u. on $p_{[100]}$ and $p_{[010]}$ axes and the deep hollow around the origin indicate that holes are doped in the x^2-y^2 and $3z^2-r^2$ orbitals.

As a first step, we have evaluated orbital occupancy as follows: Since it is essential for the analysis of the orbital state to take the hybridization between Mn-3d and O-2p orbitals into consideration, we calculated the MCP of each orbital along the observation directions using the wave functions derived from an *ab initio* molecular orbital calculation for $(MnO_6)^{8-}$ cluster,[7] and reconstructed them in the same

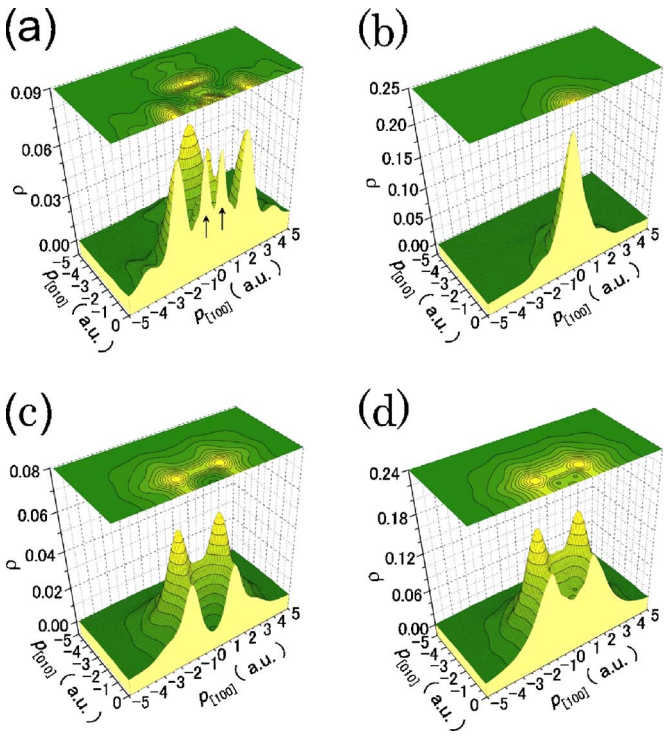

FIG. 2. (Color online) The 2D-SMD's obtained by using the result of molecular orbital calculation. The panels (a), (b), and (c) show the 2D-SMD's of x^2-y^2, $3z^2-r^2$, and t_{2g} type orbitals, respectively. (d) The reproduced 2D-SMD by fitting the calculated 2D-SMD's to the experimental one.

manner after convoluting with the experimental resolution. The calculated 2D-SMD's for x^2-y^2, $3z^2-r^2$, and t_{2g} type orbitals were best fitted to the experimental one as shown in Fig. 2, where the fully occupied t_{2g} type orbital is treated as the sum of equally populated xy, yz, and zx type ones. Since the magnetization of this system originates from the spins in Mn-3d orbitals under DE interaction, it will be reasonable to consider the spin number as the occupation number in each orbital. Therefore, the integrated intensity of the experimental 2D-SMD was normalized to a 3d electron number, 3.65, estimated from the nominal hole concentration. Then, the occupation numbers were determined from the integrated intensity of decomposed 2D-SMD's to be 0.39, 0.23, and 3.03 for x^2-y^2, $3z^2-r^2$, and t_{2g} type orbitals, respectively. The occupation of t_{2g} type orbital is almost 3. This ensures that the calculated profiles reasonably describe the hybridized orbital state. In the FM phase, the dominance of the x^2-y^2 orbital in e_g states has been pointed out by several theoretical works.[14–19] Among them, Okamoto *et al.* have parametrized the e_g orbital structure for ferromagnetic ordering with taking account of the e_g electron correlation and the energy level splitting between x^2-y^2 and $3z^2-r^2$ orbitals due to the Jahn-Teller (JT) type distortion.[15] According to this model, the scope of the parameter is from 1 to −1. The values of 1 and −1 mean the entire alignment of $3z^2-r^2$ and x^2-y^2 orbitals, respectively, and the value of 0 denotes that the two orbitals are equally populated. In the range of $0.3<x<0.475$, the parameter tends to approach an optimal value with decreasing temperature below T_c. The corresponding parameter was

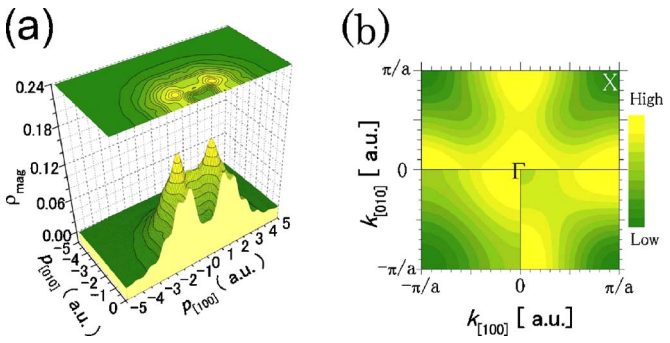

FIG. 3. (Color online) Comparison between experimental and theoretical LCW maps. (a) A theoretical 2D-SMD of all the valence bands contributing to magnetization. (b) The upper, lower left, and lower right panels are, respectively, the LCW maps derived from the experimental 2D-SMD [Fig. 1(b)], band calculation [Fig. 3(a)], and x^2-y^2 type molecular orbital [Fig. 2(a)].

estimated to be −0.26 from the present fitting result. The value is consistent with the theoretical value of −0.25 for $x=0.35$.

In the next step, we have also compared the experimental 2D-SMD to a theoretical one based on a local spin density approximation band calculation. In the calculation, we adopted a virtual crystal approximation. The Sr atom was replaced by the Ba atom, and then the La/Ba site was assumed to be occupied by the virtual atom which has a nuclear charge of 56.4. We also brought in a small U value, i.e., $U_{\mathrm{eff}}=U-J=2$ eV, for Mn $3d$ state to obtain a half metallic state. Figure 3(a) shows the 2D-SMD of all the valence bands contributing to magnetization reconstructed from the calculated MCP's after the same reconstruction procedure. It appears very similar to the experimental one in whole. Then, the Lock-Crisp-West (LCW) folding, which transforms the momentum density to an occupation-number density in the k space, was applied both to the experimental and calculated 2D-SMD's.[20] In metallic substances, a wave function is described by the Bloch function with a period of crystal lattice. Therefore, the band structure determined by the periodic potential is naturally reflected in the momentum density. In the case of two-dimensional analysis, the occupation-number density is $N(k_x,k_y)=\Sigma_{G_x,G_y}\rho(k_x+G_x,k_y+G_y)$, where the sum runs over a series of reciprocal vectors (G_x,G_y). In this study, both the experimental and calculated 2D-SMD's were divided by the size of $(2\pi/a,2\pi/a)$, where a denotes a lattice constant, and is 3.8587 Å (=7.2918 a.u.) for the crystal.[2] Then, each piece was folded back into the projected first Brillouin zone. Figure 3(b) shows both the experimental and theoretical 2D-LCW densities in the reduced zone scheme. The LCW map of t_{2g}-like bands is considered to be almost flat because of full occupancy, and thus the e_g contribution is emphasized in the figure. The electron pocket centering around the Γ point and the strip-shaped area extended along $k_{[100]}$ and $k_{[010]}$ axes are contributions from e_g-like bands, and hole pockets are found with L-shaped contour lines around the X points. However, the Fermi edge jump, which should appear as discontinuities in the LCW map, could not be found within the present momentum resolution. In spite of the similarity between the experimental and calculated 2D-SMD's, those LCW maps have a difference in density particularly around the points $(\pm\pi/a,0)$ and $(0,\pm\pi/a)$. It is hard to explain the high-density areas in the experimental LCW map only by the present band picture. The difference is likely to be caused by the molecular orbital with x^2-y^2 type symmetry. In fact, the small but sharp peaks denoted by arrows in Fig. 1(b) well reflect a feature of x^2-y^2 type molecular orbital, as can be also seen in Fig. 2(a). The hybridization effect appears on MCP as a periodic structure depending on the Mn-O bond length. Such periodic contributions of molecular orbitals would draw some pattern, and be overlapped with that of e_g bands in the LCW map. Although the LCW folding should be generally applicable to the momentum density described by the Bloch state, we tentatively applied the folding method to the 2D-SMD of x^2-y^2 type molecular orbital. In consequence, a characteristic pattern was obtained as shown in the lower right panel of Fig. 3(b), and the pattern well describes the high-density areas in the experimental LCW map. The present result indicates that a part of e_g electrons forms a band structure, and the rest may stay in a localized molecular orbital even well below T_c, suggesting a localized polaron. So far, a number of experimental and theoretical studies have pointed out the existence of polaron in this system. However, few experiments have referred to the orbital character of the polaronic state. Neutron and x-ray diffraction studies have observed charge and orbital orderings where the e_g electrons alternately occupy the $3x^2-r^2$ and $3y^2-r^2$ orbitals, and considered the orderings as an orbital polaron.[21–24] Although the ordering state disappears below T_c, we attempted to apply the LCW folding method to the $3x^2-r^2$ and $3y^2-r^2$ type molecular orbitals because MCP measurements can observe such orbital states whether they are orbitally ordered or not. The result substantially reproduces the high-density areas in Fig. 3. Therefore, it is also conceivable that the polaronic state with a mixture of $3x^2-r^2$ and $3y^2-r^2$ orbitals persists even after the collapse of orbital ordering below T_c. The reason why the localized state is described by the molecular orbitals would be related to the above-mentioned theoretical model where the localized polaron coexists with bandlike electrons.[5] In the model, the polaron goes back and forth between two adjacent Mn sites. This motion induces the ferromagnetic interaction between the two sites, and is termed a virtual double-exchange process. Since the MCP measurement is only sensitive to ferromagnetic electrons, such to-and-fro motion of e_g electrons would be observed as the molecular orbitals. In that sense, the present observation is presumably a FM polaron. Recent theoretical works, which are based on the 1D ferromagnetic Kondo model, have pointed out that the DE mechanism stabilizes a well-separated FM polaron.[25,26] Koller *et al.* have shown that the effect of the FM polaron confined to a small area appears as dispersionless structures in the spin-integrated spectral density.[25] This may give another explanation of the present observation.

In conclusion, we have visualized the orbital state of magnetic electrons in $La_{2-2x}Sr_{1+2x}Mn_2O_7$ $(x=0.35)$ in the form of 2D-SMD through the reconstruction analysis of 1D MCP's measured in a number of directions. The experimental 2D-SMD has been compared with two theoretical ones obtained by using the wave functions to come out from molecular

orbital calculation and from band calculation. The fitting analysis by using the molecular orbitals proves the dominance of x^2-y^2 type orbital in the e_g state. The localized and itinerant features of e_g type electrons are simultaneously revealed in the LCW map, suggesting the coexistence of polaronic and band states in the FM phase. The polaronic state would be attributed to the x^2-y^2 type molecular orbital or the mixed state of $3x^2-r^2$ and $3y^2-r^2$ type orbitals, while the orbitals are disordered below T_c. The e_g electronic state near T_c will sensitively vary with the temperature and external magnetic field. The 2D reconstruction of high-resolution Compton profiles will be also effective for the observation of change in the electronic state involved with the MI transition and CMR phenomenon.

We are indebted to M. Itou and Y. Sakurai for assistance in MCP measurements on the beam line 08 W at SPring-8, Japan. We also thank Y. Tanaka and S. Miyaki for technical advice on the reconstruction analysis and molecular orbital calculation, respectively. The computational code (BANDS01) of band calculation used here was originally developed by A. Kodama, N. Hamada, and A. Yanase. The synchrotron-radiation experiments were performed with the approval of the Japan Synchrotron Radiation Research Institute (JASRI) (Proposal No. 2002A0008-LD3-np). This work was supported in part by a Grant-in-Aid for Scientific Research from the Ministry of Education, Science, Sports and Culture, Japan, and by Hyogo Science and Technology Association.

[1] R. von Helmolt, J. Wecher, B. Holzapfel, L. Schultz, and K. Samwer, Phys. Rev. Lett. **71**, 2331 (1993); S. Jin, T. H. Tiefel, M. McCormack, R. A. Fastnacht, R. Ramesh, and L. H. Chen, Science **264**, 413 (1994); A. Urushibara, Y. Moritomo, T. Arima, A. Asamitsu, G. Kido, and Y. Tokura, Phys. Rev. B **51**, 14103 (1995); Y. Moritomo, A. Asamitsu, H. Kuwahara, and Y. Tokura, Nature (London) **380**, 141 (1996).

[2] M. Kubota, H. Fujioka, K. Hirota, K. Ohoyama, Y. Moritomo, H. Yoshizawa, and Y. Endoh, J. Phys. Soc. Jpn. **69**, 1606 (2000).

[3] C. Zener, Phys. Rev. **82**, 403 (1951); P. W. Anderson and H. Hasegawa, *ibid.* **100**, 675 (1955); P. G. de Gennes, *ibid.* **118**, 141 (1960).

[4] Y. Tokura and Y. Tomioka, J. Magn. Magn. Mater. **200**, 1 (1999); A. J. Millis, P. B. Littlewood, and B. I. Shraiman, Phys. Rev. Lett. **74**, 5144 (1995); T. Mizokawa and A. Fujimori, Phys. Rev. B **56**, R493 (1997); H. Koizumi, T. Hotta, and Y. Takada, Phys. Rev. Lett. **80**, 4518 (1998).

[5] T. V. Ramakrishnan, H. R. Krishnamurthy, S. R. Hassan, and G. Venketeswara Pai, Phys. Rev. Lett. **92**, 157203 (2004).

[6] S. Miyaki, S. Uzuhara, K. Terada, K. Makoshi, and H. Koizumi, Phys. Rev. B **71**, 085117 (2005).

[7] A. Koizumi, S. Miyaki, Y. Kakutani, H. Koizumi, N. Hiraoka, K. Makoshi, N. Sakai, K. Hirota, and Y. Murakami, Phys. Rev. Lett. **86**, 5589 (2001); A. Koizumi, T. Nagao, Y. Kakutani, N. Sakai, K. Hirota, and Y. Murakami, Phys. Rev. B **69**, 060401(R) (2004); A. Koizumi, T. Nagao, Y. Kakutani, N. Hiraoka, N. Sakai, T. Arima, K. Hirota, and Y. Murakami, J. Phys. Chem. Solids **66**, 2183 (2005).

[8] Y. Li, P. A. Montano, J. F. Mitchell, B. Barbiellini, P. E. Mijnarends, S. Kaprzyk, and A. Bansil, Phys. Rev. Lett. **93**, 207206 (2004).

[9] B. Barbiellini, P. E. Mijnarends, S. Kaprzyk, A. Bansil, Y. Li, J. F. Mitchell, and P. A. Montano, J. Phys. Chem. Solids **66**, 2197 (2005).

[10] M. J. Cooper, P. E. Mijnarends, N. Shiotani, N. Sakai, and A. Bansil, *X-ray Compton Scattering* (Oxford University Press, New York, 2004).

[11] Y. Tanaka, N. Sakai, Y. Kubo, and H. Kawata, Phys. Rev. Lett. **70**, 1537 (1993); L. Dobrzynski and E. Zukowski, J. Phys.: Condens. Matter **11**, 8049 (1999).

[12] K. Hirota, Y. Moritomo, H. Fujioka, M. Kubota, H. Yoshizawa, and Y. Endoh, J. Phys. Soc. Jpn. **67**, 3380 (1998).

[13] Y. Tanaka, K. J. Chen, C. Bellin, G. Loupias, H. M. Fretwell, A. R. Gonzalez, M. A. Alam, S. B. Dugdale, A. A. Manuel, A. Shukla, T. Buslaps, P. Suortti, and N. Shiotani, J. Phys. Chem. Solids **61**, 365 (2000); Y. Tanaka, Y. Sakurai, A. T. Stewart, N. Shiotani, P. E. Mijnarends, S. Kaprzyk, and A. Bansil, Phys. Rev. B **63**, 045120 (2001).

[14] S. Yunoki, T. Hotta, and E. Dagotto, Phys. Rev. Lett. **84**, 3714 (2000).

[15] S. Okamoto, S. Ishihara, and S. Maekawa, Phys. Rev. B **63**, 104401 (2001).

[16] G. Jackeli and N. B. Perkins, Phys. Rev. B **65**, 212402 (2002).

[17] A. M. Olés and L. F. Feiner, Phys. Rev. B **67**, 092407 (2003).

[18] Q. Zhang, W. Zhang, and Z. Jiang, Phys. Rev. B **72**, 142401 (2005).

[19] M. Daghofer, A. M. Olés, D. N. Neuber, and W. von der Linden, Phys. Rev. B **73**, 104451 (2006).

[20] D. G. Lock, V. H. C. Crisp, and R. N. West, J. Phys. F: Met. Phys. **3**, 561 (1973).

[21] S. Shimomura, N. Wakabayashi, H. Kuwahara, and Y. Tokura, Phys. Rev. Lett. **83**, 4389 (1999).

[22] L. Vasiliu-Doloc, S. Rosenkranz, R. Osborn, S. K. Sinha, J. W. Lynn, J. Mesot, O. H. Seeck, G. Preosti, A. J. Fedro, and J. F. Mitchell, Phys. Rev. Lett. **83**, 4393 (1999).

[23] M. Kubota, H. Yoshizawa, Y. Moritomo, H. Fujioka, K. Hirota, and Y. Endoh, J. Phys. Soc. Jpn. **68**, 2202 (1999).

[24] B. J. Campbell, S. K. Sinha, R. Osborn, S. Rosenkranz, J. F. Mitchell, D. N. Argyriou, L. Vasiliu-Doloc, O. H. Seeck, and J. W. Lynn, Phys. Rev. B **67**, 020409(R) (2003).

[25] W. Koller, A. Prüll, H. G. Evertz, and W. von der Linden, Phys. Rev. B **67**, 174418 (2003).

[26] D. N. Neuber, M. Daghofer, H. G. Evertz, and W. von der Linden, Phys. Rev. B **73**, 014401 (2006).